

Solvent Effects on Uranium(VI) Fluoride and Hydroxide Complexes Studied by EXAFS and Quantum Chemistry

Valérie Vallet,^{*,†} Ulf Wahlgren,[†] Bernd Schimmelpfennig,[‡] Henry Moll,[§] Zoltán Szabó,^{||} and Ingmar Grenthe^{*,||}

Institute of Physics, Stockholm University, P.O. Box 6730, S-11385 Stockholm, Sweden, Theoretical Chemistry, Department of Chemistry, Royal Institute of Technology (KTH), S-10044 Stockholm, Sweden, Institute of Radiochemistry, Forschungszentrum Rossendorf e.V., P.O. Box 510119, D-01314 Dresden, Germany, and Inorganic Chemistry, Department of Chemistry, Royal Institute of Technology (KTH), S-100 44 Stockholm, Sweden

Received December 12, 2000

The structures of the complexes $\text{UO}_2\text{F}_n(\text{H}_2\text{O})_{5-n}^{2-n}$, $n = 3-5$, have been studied by EXAFS. All have pentagonal bipyramid geometry with U–F of and U–H₂O distances equal to 2.26 and 2.48 Å, respectively. On the other hand the complex $\text{UO}_2(\text{OH})_4^{2-}$ has a square bipyramid geometry both in the solid state and in solution. The structures of hydroxide and fluoride complexes have also been investigated with wave function based and DFT methods in order to explore the possible reasons for the observed structural differences. These studies include models that describe the solvent by using a discrete second coordination sphere, a model with a spherical, or shape-adapted cavity in a conductor-like polarizable continuum medium (CPCM), or a combination of the two. Solvent effects were shown to give the main contribution to the observed structure variations between the uranium-(VI) tetrahydroxide and the tetrafluoride complexes. Without a solvent model both $\text{UO}_2(\text{OH})_4(\text{H}_2\text{O})^{2-}$ and $\text{UO}_2\text{F}_4(\text{H}_2\text{O})^{2-}$ have the same square bipyramid geometry, with the water molecule located at a distance of more than 4 Å from uranium and with a charge distribution that is very near identical in the two complexes. Of the models tested, only the CPCM ones are able to describe the experimentally observed square and pentagonal bipyramid geometry in the tetrahydroxide and tetrafluoride complexes. The geometry and the relative energy of different isomers of $\text{UO}_2\text{F}_3(\text{H}_2\text{O})_2^-$ are very similar, indicating that they are present in comparable amounts in solution. All calculated bond distances are in good agreement with the experimental observations, provided that a proper model of the solvent is used.

The common coordination geometry of uranium(VI) complexes with small ligands is a pentagonal bipyramid, with all labile ligands in the plane perpendicular to the linear UO_2 unit. The $\text{UO}_2(\text{OH})_4^{2-}$ complex is an exception, having a square bipyramid geometry in the solid state.¹ The corresponding tetrafluoride complex has also been studied in the solid state using single-crystal X-ray diffraction² and was found to have the more common pentagonal bipyramid geometry by coordination of H_2O . The same structures seem to be retained also in solution, as indicated by EXAFS data for the hydroxide system^{1,3,4} and data on the fluoride system presented in this study. The difference between the two systems is surprising in view of the chemical similarity between hydroxide and fluoride,

with numerous examples of isomorphic substitutions between OH^- and F^- in the solid state. In one of our previous investigations we used quantum chemical methods as a tool to obtain a more detailed insight into the structure and dynamics of solution chemical systems.⁴ In this study we will explore the chemistry of the U(VI)–fluoride system using EXAFS and previous X-ray data.² We will also compare the structure and bonding in uranium(VI) fluoride and hydroxide complexes by using different wave function and DFT based methods, both with and without the inclusion of models for the solvent. Solvent models are important because there are significant differences in the hydrogen bonding of OH^- and F^- , where the former can act both as donor and as acceptor, the latter only as an acceptor, which may explain the observed chemical differences. We will begin our discourse with a presentation of new and older experimental results and then continue with a theory section and a discussion.

Experimental Investigations, Methods, and Results

EXAFS Measurements. U(VI) perchlorate stock solutions were prepared as described before.⁵ Appropriate aliquots were taken to obtain the 0.05 M test solutions B, C, and D. Their fluoride concentrations, 0.21, 0.45, and 3.00 M, respectively, were adjusted by adding NaF (solutions B and C) or tetramethylammonium fluoride (solution D).

* Authors to whom correspondence should be addressed. I.G.: e-mail, ingmarg@inorg.kth.se; fax, +46-8-212626. V.V.: e-mail, vallet@physto.se; fax, +46-8-347817.

[†] Institute of Physics, Stockholm University.

[‡] Theoretical Chemistry, Department of Chemistry, Royal Institute of Technology.

[§] Institute of Radiochemistry, Forschungszentrum Rossendorf e.V.

^{||} Inorganic Chemistry, Department of Chemistry, Royal Institute of Technology.

(1) Clark, D. L.; Conradson, S. D.; Donohoe, R. J.; Keogh, R. J.; Morris, D. E.; Palmer, P. D.; Rogers, R. D.; Tait, C. D. *Inorg. Chem.* **1999**, *38*, 1456.

(2) Mak, T. C. W.; Yip, W.-H. *Inorg. Chim. Acta* **1985**, *109*, 131.

(3) Moll, H.; Reich, T.; Szabó, Z. *Radiochim. Acta* **2000**, *88*, 411.

(4) Wahlgren, U.; Moll, H.; Grenthe, I.; Schimmelpfennig, B.; Maron, L.; Vallet, V.; Gropen, O. *J. Phys. Chem. A* **1999**, *103*, 8257.

(5) Ciavatta, L.; Ferri, D.; Grenthe, I.; Salvatore, F. *Inorg. Chem.* **1981**, *20*, 463.

Table 1. EXAFS Data for the Structures of $\text{UO}_2(\text{H}_2\text{O})_5^{2+}$ and $\text{UO}_2\text{F}_n(\text{H}_2\text{O})_{5-n}^{2-n}$ Complexes in Solution

sample/U(VI) speciation	model	shell	N	R (Å)	σ^2 (Å ²)	ΔE_0 (eV)	res	ref
A 0.05 M UO_2^{2+} in 0.1 M HClO_4	2-shell fit	U–O _{ax} U–O _{eq}	2.0 ^a 5.2 ± 0.4	1.77 2.41	0.0012 0.0061	–16.0	0.22	4
B 0.052 M UO_2^{2+} , 0.21 M F^- , pH 5.0	2-shell fit	U–O _{ax} U–O _{eq}	2.0 ^a 3.5 ± 0.6	1.79 2.26	0.0016 0.0042	–16.7	0.21	this work
C 0.052 M UO_2^{2+} , 0.45 M F^- , pH 5.3	3-shell fit	U–O _{ax}	2.0 ^a	1.80	0.0016	–15.0	0.19	this work
		U–F	3.5 ± 0.7	2.25	0.0046			
		U–O _{eq}	1.5 ^a	2.47	0.0057			
D $\text{UO}_2\text{F}_5^{3-}$	2-shell fit	U–O _{ax} U–O _{eq}	2.0 ^a 4.8 ± 0.6	1.79 2.27	0.0016 0.0049	–17.3	0.19	this work
	3-shell fit	U–O _{ax}	2.0 ^a	1.80	0.0016	–15.0	0.12	
		U–F	4.1 ± 0.7	2.26	0.0048			
		U–O _{eq}	1.0 ^a	2.48	0.0046			

^a Parameter fixed during the fit. $\sigma R = \pm 0.006$ Å.

The $-\log [\text{H}^+]$ of the test solutions was adjusted using NaOH and/or HClO_4 . The path length of the solutions B and C was 13 mm, which gave an edge jump of 1.0 across the U L_{III} absorption edge. The path length of solution D was approximately 40 mm.

The EXAFS transmission spectra were measured at room temperature using a water-cooled Si(111) double-crystal monochromator of fixed exit ($E = 5-35$ keV) at the Rossendorf Beamline (ROBL) at ESRF, Grenoble. Higher harmonics were rejected using two Si- and Pt-coated mirrors. More information about the EXAFS measurements can be found in ref 6. Three scans were averaged from samples B and C and four from sample D. Zr (samples B and C) and Y (sample D) foils were used for the energy calibration. The ionization energy of the U L_{III} electron, E_0 , was defined as 17185 eV. The data were treated using the EXAFSPAK⁷ software. Theoretical backscattering phase and amplitude functions used in data analysis were calculated for the model complexes $\text{UO}_2\text{F}_4(\text{H}_2\text{O})_2^{2-}$ and $\text{UO}_2\text{F}_5^{3-}$ using the known crystal structures^{2,8} and the FEFF7 program.⁹ The MS path O–U–O (four-legged path) of the linear UO_2^{2+} unit was included in the model fitting. The EXAFS oscillations were isolated using standard procedures for preedge subtraction, spline removal, and data normalization.⁹ The amplitude reduction factor, S_0^2 , was held constant at 0.9 for all the fits.

The bond lengths and coordination numbers obtained are summarized in Table 1. The EXAFS spectra and the corresponding Fourier transforms (FT) are shown in Figure 1. The EXAFS oscillations of U(VI) are very similar at the different fluoride concentrations, but differ from those observed in the acid $\text{UO}_2^{2+}(\text{aq})$ sample A.⁴ The differences are more pronounced in the FT's (which are not corrected for the EXAFS phase shift).

The refinement of the EXAFS data was made using models with two or three shells, cf. Table 1. For solutions B and C the two-shell model gives a U–O_{ax} first-shell distance in good agreement with those commonly found for the UO_2 unit, and a second-shell U–(O,F) distance that agrees with the known U–F distance in crystal structures.^{2,8,10,11} However, the number of bond distances in the second shell, N , is not consistent with the known coordination number in the equatorial plane of U(VI). The large value of the residual in the two-shell model indicates that it is incomplete. The three-shell model gives a significant decrease

in the residual and bond distances and coordination numbers in excellent agreement with the known distances U–F and U–H₂O^{2,8,10,11} and the known composition of the test solutions, cf. Table 1. In previous EXAFS studies^{1,3,4} of $\text{UO}_2(\text{OH})_4^{2-}$ there was no indication of third-shell interactions. The small backscattering from oxygen and the interference of the two equatorial shells makes it difficult to estimate a precise value of the number of coordinated water molecules. In the final refinement of the data from solutions B and C we have therefore assumed that this is equal to $(5 - n_F)$, where n_F is the average number of coordinated fluorides. This value, precisely known from the equilibrium constants¹² and total concentration of uranium and fluoride in the test solutions, was used as a fixed parameter in the final fitting of the EXAFS data. A calculation with a floating amplitude reduction factor gave $S_0^2 = 0.93$, confirming that the structure model used is reasonable. Test solutions B and C contain a mixture of $\text{UO}_2\text{F}_3(\text{H}_2\text{O})_2^{2-}$ and $\text{UO}_2\text{F}_4(\text{H}_2\text{O})_2^{2-}$, but the data do not indicate a significant difference in the U–F and U–H₂O distances between the complexes. In solution D the two-shell model is satisfactory and results in U–F distances in close agreement with those found in solid-state structures.

Quantum Chemical Calculations, Methods, and Results

The DFT and wave function based calculations have been made using various approximations to obtain information on the structure of the different fluoride complexes, their relative energy in the gas phase, and how the solvent affects them. Most of the wave function based calculations were carried out using the Molcas 5 program package.¹³ By replacing the core electrons by a relativistic ECP (effective core potential) we could achieve a significant reduction in the size of the computation. Previous studies^{14–16} have shown that the accuracy of the energy consistent ECPs of Stuttgart-type^{17,18} at the correlated level is

- (6) Matz, W.; Schell, N.; Bernhard, G.; Prokert, F.; Reich, T.; Clausner, J.; Oehme, W.; Schlenk, R.; Diemel, S.; Funke, H.; Eichhorn, F.; Betzl, M.; Pröhl, D.; Strauch, U.; Hüttig, G.; Krug, H.; Newmann, W.; Brendler, V.; Reichel, P.; Denecke, M. A.; Nitsche, H. *J. Synchrotron Rad.* **1999**, *6*, 1076.
- (7) George, G. N.; Pickering, I. J. 1995. EXAFSPAK, A suite of computer programs for analysis of X-ray absorption spectra. Stanford Synchrotron Radiation Laboratory, Stanford, USA.
- (8) Zachariassen, W. H. *Acta Crystallogr.* **1954**, *7*, 783.
- (9) Zabinski, S. I.; Rehr, J. J.; Ankudinov, A.; Albers, R. C.; Eller, M. J. *Phys. Rev. B* **1995**, *52*, 2995.
- (10) Pepper, M.; Bursten, B. E. *Chem. Rev.* **1991**, *91*, 719.
- (11) Farkas, I.; Csöregy, I.; Szabó, Z. *Acta Chem. Scand.* **1999**, *53*, 1009.

- (12) Grenthe, I.; Fuger, J.; Konings, R. J. M.; Lemire, R. J.; Muller, A. B.; Nguyen-Trung, C.; Wanner, H. *Chemical Thermodynamics of Uranium*; North-Holland: Amsterdam, 1992.
- (13) Andersson, K.; Barysz, M.; Bernhardsson, A.; Blomberg, M. R. A.; Cooper, D. L.; Fleig, T.; Fülcher, M. P.; de Graaf, C.; Hess, B. A.; Karlström, G.; Lindh, R.; Malmqvist, P.-A.; Neogrády, P.; Olsén, J.; Roos, B. O.; Sadlej, A. J.; Schütz, M.; Schimmelpfennig, B.; Seijo, L.; Serrano-Andrés, L.; Siegbahn, P. E. M.; Stålring, J.; Thorsteinsson, T.; Veryazov, V.; Widmark, P.-O. *MOLCAS Version 5*. Lund University, Sweden 2000.
- (14) Vallet, V.; Schimmelpfennig, B.; Maron, L.; Teichteil, C.; Leininger, T.; Grenthe, I.; Wahlgren, U. *Chem. Phys.* **1999**, *244*, 185.
- (15) Vallet, V.; Maron, L.; Schimmelpfennig, B.; Leininger, T.; Teichteil, C.; Gropen, O.; Grenthe, I.; Wahlgren, U. *J. Phys. Chem. A* **1999**, *103*, 9285.
- (16) Vallet, V.; Schimmelpfennig, B.; Maron, L.; Leininger, T.; Teichteil, C.; Gropen, O.; Wahlgren, U. **2000**, to be submitted.

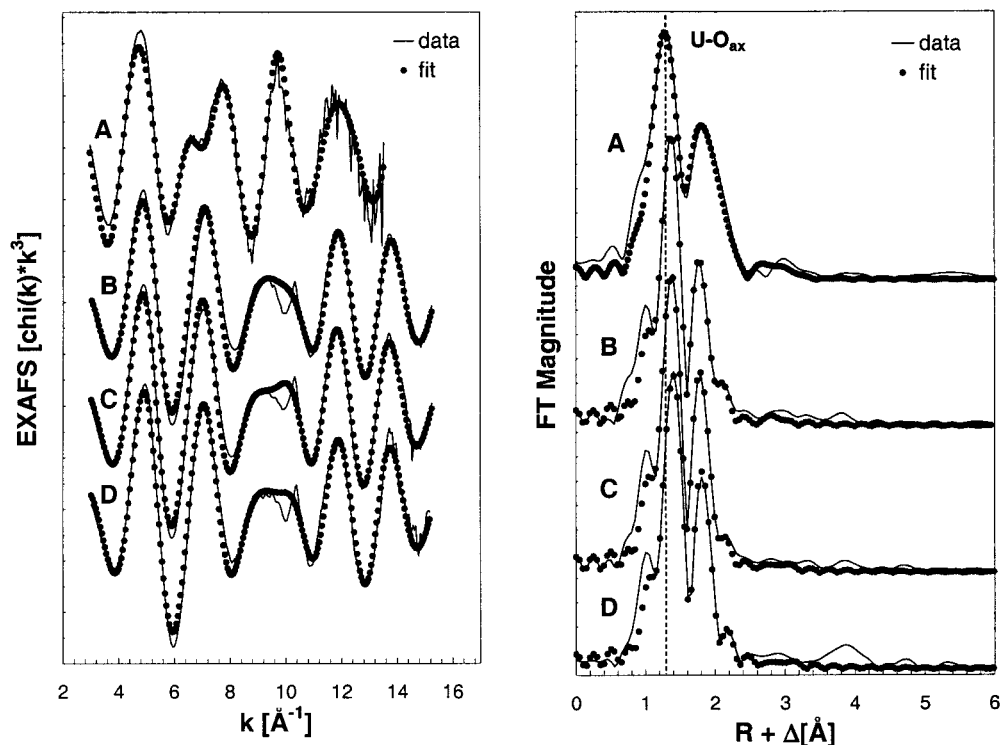


Figure 1. U L_{III} -edge k^3 -weighted EXAFS data and corresponding FT's measured for the following samples: (A) 0.05 M UO_2^{2+} in 0.1 M $HClO_4$, (B) 0.052 M UO_2^{2+} + 0.21 M F^- (pH = 5.0), (C) 0.052 M UO_2^{2+} + 0.45 M F^- (pH = 5.3), and (D) a sample containing $UO_2F_5^{3-}$. The solid line is the experimental data, and the dashed line represents the best theoretical fit of the data.

excellent, hence we used these for both uranium and the ligands, except for the hydrogen atoms, which were described by Huzinaga's 5s basis contracted to 3s, with one additional diffuse p-function (exponent 1.0).

The geometry of all the compounds was optimized at the SCF level using gradient techniques, some with symmetry constraints. Correlation effects were estimated at the MP2 level by single-point calculations at the SCF optimized geometry, without correlating the 5s, 5p, and 5d shells on uranium. We investigated the structure of complexes with a different number of coordinated water molecules and fluoride ions and of isomers with different location and orientation of the water molecules in the first and second coordination spheres. For the isomers of $UO_2F_4(H_2O)^{2-}$, we compared the wave function based results obtained with Molcas 5 with those obtained from the density functional theory (DFT) approach in Gaussian 98¹⁹ using the hybrid functional B3LYP^{20,21} and the same RECPs and basis sets as in the wave function based calculation. The symmetry constraints used in geometry optimizations are indicated in the

tables. Solvent effects were estimated using three models. In the first we added a small number of water molecules in a second coordination sphere to represent the solvent; in the second the solvent was represented by a dielectric continuum of permittivity $\epsilon_0 = 80$, while the third was a combination of the two. Various implementations of the continuum model exist, which differ by the shape of the cavity used and by the treatment of the various contributions to the solvation energy derivatives. No gradients of the solvation energies have been implemented in the Molcas 5²² reaction field model. It uses a simple sphere cavity, the position and size of which cannot be optimized automatically. Gaussian 98 offers the possibility to use the more elaborated conductor-like polarizable continuum model (CPCM),²³ where the form of the cavity matches the shape of the molecule and where electrostatic and nonelectrostatic terms are included in the solvation energy derivatives. The method allows both single-point calculations and geometry optimization using gradients within the bulk model; a detailed description is given in ref 23.

The coordinates for the various structures are given in the Supporting Information, Table S1.

Structures of $UO_2F_4^{2-}$ and $UO_2F_4(H_2O)^{2-}$ in the Gas Phase (No Solvent Model). The optimized geometry of $UO_2F_4^{2-}$ and the three isomers of $UO_2F_4(H_2O)^{2-}$ at the SCF and B3LYP levels are given in Table 2 and perspective views of structures 1 and 2 in parts a and b of Figure 2 and of structure 3 in the Supporting Information; their corresponding energy differences are shown in Table 3, and the order of increasing stability is structure 1 < structure 3 < structure 2. Both the SCF and the B3LYP calculations give the same relative order among the three structures and very similar energies. Structure 1 is the only one with coordinated water and has its hydrogen atoms pointing toward the neighboring fluoride ions. In structure

(17) Küchle, W.; Dolg, M.; Stoll, H.; Preuss, H. *J. Chem. Phys.* **1994**, *100*, 7535.

(18) Bergner, A.; Dolg, M.; Küchle, W.; Stoll, H.; Preuss, H. *J. Mol. Phys.* **1993**, *80*, 1431.

(19) Gaussian 98 (Revision A.7), Frisch, M. J.; Trucks, G. W.; Schlegel, H. B.; Scuseria, G. E.; Robb, M. A.; Cheeseman, J. R.; Zakrzewski, V. G.; Montgomery, J. A.; Stratmann, R. E.; Burant, J. C.; Dapprich, S.; Millam, J. M.; Daniels, A. D.; Kudin, K. N.; Strain, M. C.; Farkas, O.; Tomasi, J.; Barone, V.; Cossi, M.; Cammi, R.; Mennucci, B.; Pomelli, C.; Adamo, C.; Clifford, S.; Ochterski, J.; Petersson, G. A.; Ayala, P. Y.; Cui, Q.; Morokuma, K.; Malick, D. K.; Rabuck, A. D.; Raghavachari, K.; Foresman, J. B.; Cioslowski, J.; Ortiz, J. V.; Stefanov, B.; Liu, G.; Liashenko, A.; Piskorz, P.; Komaromi, I.; Gomperts, R.; Martin, R. L.; Fox, D. J.; Keith, T.; Al-Laham, M. A.; Peng, C. Y.; Nanayakkara, A.; Gonzalez, C.; Challacombe, M.; Gill, P. M. W.; Johnson, B. G.; Chen, W.; Wong, M. W.; Andres, J. L.; Head-Gordon, M.; Replogle, E. S.; Pople, J. A. Gaussian, Inc., Pittsburgh, PA, **1998**.

(20) Becke, A. D. *J. Chem. Phys.* **1993**, *98*, 5648.

(21) Lee, C.; Yang, W.; Parr, R. G. *Phys. Rev. B* **1988**, *37*, 785.

(22) Karlström, G. *J. Phys. Chem.* **1988**, *92*, 1315.

(23) Barone, V.; Cossi, M.; *J. Phys. Chem. A* **1998**, *102*, 1995.

Table 2. Calculated and Experimental Bond Distances (Å) for Uranyl Fluoride Complexes in the Solid State and in Solution^a

chemical species	structure of complex (sym)	method	U–O _{yl} (Å) [OUO angle]	U–F (Å)	U–H ₂ O (Å)
UO ₂ F ₄ (H ₂ O) ²⁻ (aq)		EXAFS, this study	1.80	2.26	2.48
UO ₂ F ₄ (H ₂ O) ²⁻ (solid) (cf. Discussion)		X-ray, ref 2	1.780	2.28–2.39 (two dist)	2.110
UO ₂ F ₄ ²⁻	(D _{4h})	SCF gas phase	1.754	2.258	2.748
UO ₂ F ₄ (H ₂ O) ²⁻	struct 1, Fig. 2a (C _{2v})	SCF gas phase B3LYP SCF + CPCM	1.740 [177.5] 1.822 [177.5] 1.751 [179.2]	2.248–2.335 2.216–2.305 2.255–2.264	2.748 2.730 2.619
UO ₂ F ₄ (H ₂ O) ²⁻ (water in the plane at long distance)	struct 2, Fig. 2b (C _{2v})	SCF gas phase B3LYP SCF + CPCM	1.736 [179.9] 1.818 [179.9] 1.745 [180.0]	2.246–2.281 2.225–2.267 2.226–2.250	4.081 3.980 4.071
UO ₂ F ₄ (H ₂ O) ²⁻ (water out of the plane at long distance)	struct 3 (C _{2v})	SCF gas phase B3LYP SCF + CPCM	1.739 [179.9] 1.823 [179.9] 1.749 [179.5]	2.249–2.256 2.20–2.290 2.227–2.334	4.490 4.312 4.880
UO ₂ F ₅ ³⁻	struct 4 (D _{5h})	SCF gas phase CPCM EXAFS	1.764 1.759 1.80	2.345 2.292 2.26	

^a The calculations have been made with symmetry constraints as indicated in this and the following tables. The different structures are shown in Figure 2 and in the Supporting Information. The solvent is described using the CPCM model.

Table 3. Relative Stability of the Three Isomers of UO₂F₄(H₂O)²⁻ in the Gas Phase and in the Solvent^a

complex	method	UO ₂ F ₄ (H ₂ O) ²⁻		
		coordinated water	water in the plane at long distance	water out of the plane at long distance
bare complex	structure no.	1	2	3
	gas phase	0.00	–138.8	–99.6
	B3LYP	0.00	–149.0	–110.0
	spherical cavity	0.00	+3.9	+50.8
	single point (cavity size)	(3.43 Å)	(4.47 Å)	(4.81 Å)
	CPCM single point	0.00	+39.9	+55.6
	CPCM geom opt	0.00	+10.1	+23.6
complex + second coordination shell	structure no.	10	11	12
	gas phase	0.00	–83.7	–52.3
	spherical cavity	0.00	–57.2	–4.18
	single point (cavity size)	(5.18 Å)	(5.16 Å)	(5.42 Å)
	CPCM single point ^b	0.00	+9.0	+18.9

^a All energies in kJ/mol and calculated at the MP2 and B3LYP levels. ^b Energies at the SCF level as MP2 calculations could not be handled.

2, the water molecule is located in the second coordination sphere, also with the hydrogen atoms pointing toward fluoride ions. In structure 3, the plane of the water in the second coordination sphere is perpendicular to the equatorial plane. Both structures 2 and 3 are clearly four-coordinated, with the water molecule well outside the known experimental coordinating bond distances.

We investigated the influence of correlation effects by reoptimizing the various structures at the DFT level, using the hybrid functional B3LYP. The internal uranyl distances agree within 0.02 Å with experiment, but are 0.1 Å longer than those at the SCF level, the uranyl bond being always close to linear. This effect of correlation on the axial bonding was already noticed on the bare uranyl ion.¹⁴ The U–F distance is 0.02 Å shorter than at the SCF level, indicating a small effect of correlation on the metal–ligand bonding. When solvent models are included, there is a large change in the relative energy of the different structures, as discussed in the following.

The Structure of UO₂(OH)₄²⁻ in the Gas Phase and Solvent. This complex has been studied previously⁵ using the AIMP method of Huzinaga et al.^{24,25} We reoptimized the geometry of the various isomers of the uranyl hydroxide

complex in order to make a systematic comparison with the corresponding fluoride complexes. The agreement between the old AIMP results and the ECP ones is satisfactory, although the bond distances to the hydroxides calculated with the energy consistent ECPs in Table 4 are 0.04 Å shorter than the previous values.

Most of the calculations on UO₂(OH)₄²⁻ in a solvent have been made in a conformation where all the hydroxide groups are constrained to the equatorial plane (structure 5a, cf. Supporting Information). In the gas phase, this is not a true minimum as a frequency analysis leads to four imaginary frequencies corresponding to the motion of the hydroxide groups out of the equatorial plane. The stable geometry has a trans configuration (structure 5b, cf. Supporting Information) with two hydroxides up and two down and lies 55.3 and 53.0 kJ/mol below the planar structure in the gas phase and solvent, respectively (cf. Table 5). This corresponds to a rotational barrier of 13.8 kJ/mol per hydroxide group. The conformations have been studied in more detail by Schreckenbach et al.,²⁶ and they also predicted the trans conformation to be the most stable one. The agreement between their study, obtained with large core relativistic ECPs²⁷ and the hybrid functional B3LYP and ours is good. In order to test if symmetry constraints have a noticeable effect on bond distances and relative energies, we allowed the

(24) Huzinaga, S.; Seijo, L.; Barandiarán, J.; Klubokowski, M. *J. Chem. Phys.* **1987**, *86*, 2132.

(25) Huzinaga, S.; Seijo, L.; Barandiarán, J. *J. Chem. Phys.* **1989**, *91*, 7011.

Table 4. Calculated and Experimental Bond Distances of $\text{UO}_2(\text{OH})_4^{2-}$, $\text{UO}_2(\text{OH})_4(\text{H}_2\text{O})^{2-}$, and $\text{UO}_2(\text{OH})_5^{3-}$ ^a

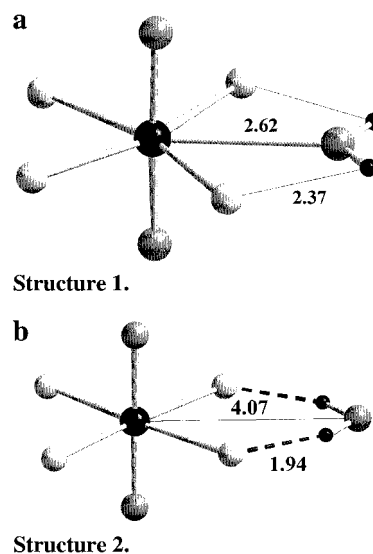
chemical species	complex (sym)	method	U–O _{yl} (Å) [OUO angle]	U–OH (Å)	U–H ₂ O (Å)
$\text{UO}_2(\text{OH})_4^{2-}$ (aq)		EXAFS, refs 1, 3, 4	1.83 ₀	2.26 ₆	
$\text{UO}_2(\text{OH})_4^{2-}$ (struct)		X-ray, ref 1	1.81 ₅	2.26 ₁	
$\text{UO}_2(\text{OH})_4^{2-}$ (hydroxide in plane)	struct 5a (C_{4h})	SCF gas phase	1.750	2.361	
$\text{UO}_2(\text{OH})_4^{2-}$ (trans “2 up, 2 down”)	struct 5b (D_{2d})	SCF gas phase	1.763	2.336	
$\text{UO}_2(\text{OH})_4(\text{H}_2\text{O})^{2-}$	struct 6a Fig. 3a (C_{2v})	SCF gas phase	1.738 [178.5]	2.387–2.416	2.611
		CPCM	1.764 [178.6]	2.339–2.360	2.593
$\text{UO}_2(\text{OH})_4(\text{H}_2\text{O})^{2-}$ (trans “1 up, 1 down”)	struct 6b Fig. 3b (C_s)	SCF gas phase	1.744	2.358–2.438	2.613
$\text{UO}_2(\text{OH})_4(\text{H}_2\text{O})^{2-}$ (water in the plane at long distance)	struct 7a (C_{2v})	SCF gas phase	1.737 [179.3]	2.353–2.356	4.081
		CPCM	1.763	2.287–2.321	3.977
$\text{UO}_2(\text{OH})_4(\text{H}_2\text{O})_2^{2-}$ (trans “2 up, 2 down”; water in the plane at long distance)	struct 7b Fig. 3c (C_s)	SCF gas phase	1.750	2.313–2.357	4.113
$\text{UO}_2(\text{OH})_4(\text{H}_2\text{O})^{2-}$ (water out of the plane at long distance)	struct 8 (C_{2v})	SCF gas phase	1.740 [179.2]	2.347	4.582
		CPCM	1.762 [179.6]	2.286–2.321	3.971
$\text{UO}_2(\text{OH})_5^{3-}$	struct 9 (C_{5h})	SCF gas phase	1.756	2.473	
		CPCM	1.775	2.387	

^a Structures optimized at the SCF level. The different structures are shown in Figure 3 and the Supporting Information.

Table 5. The MP2 Energies (kJ/mol) Relative to the Planar $\text{UO}_2(\text{OH})_4^{2-}$ and $\text{UO}_2(\text{OH})_4(\text{H}_2\text{O})^{2-}$ for Two Uranyl Tetrahydroxide Isomers, Calculated Using the Geometries in the Gas Phase and with the CPCM Solvent Model

complex	gas phase/SCF geometry	CPCM/SCF geometry
$\text{UO}_2(\text{OH})_4^{2-}$ (hydroxide in the plane) struct 5a	0	0
$\text{UO}_2(\text{OH})_4^{2-}$ (trans “2 up, 2 down”) struct 5b	–55.3	–53.0
$\text{UO}_2(\text{OH})_4(\text{H}_2\text{O})^{2-}$ struct 6a	0	
$\text{UO}_2(\text{OH})_4(\text{H}_2\text{O})^{2-}$ (trans “1 up, 1 down”) struct 6b	–26.02	
$\text{UO}_2(\text{OH})_4(\text{H}_2\text{O})^{2-}$ (water in the plane at long distance) struct 7a	0	
$\text{UO}_2(\text{OH})_4(\text{H}_2\text{O})_2^{2-}$ (trans “2 up, 2 down”; water in the plane at long distance) struct 7b	–64.56	

hydroxide groups to rotate out of the equatorial plane in the various isomers of $\text{UO}_2(\text{OH})_4(\text{H}_2\text{O})^{2-}$ in the gas phase. Structure 7b (Figure 3c) with a long-distance water is now 134.4 kJ/mol more stable than the five-coordinated structure 6b (Figure 3b), as compared to the 95.5 kJ/mol when the hydroxide groups are constrained into the plane (Table 6). Moreover the hydroxide groups adjacent to the water molecule in structure 6b rotate into the equatorial plane. The bond distances in the planar and out-of-plane structures are nearly the same. From these observations, we conclude that the planar structure is a satisfactory approximation for the calculation of bond distances and relative energies for the different tetrahydroxide structures in the gas phase. As there are only minor changes in bond distance in

**Figure 2.** Uranium(VI) tetrafluoride isomers with structures 1 (a) and 2 (b) in the CPCM model. The uranium atom and the hydrogen atoms are black; the fluoride atoms are light gray, and the oxygen atom is medium gray. The thin lines denote the distance between nonbonded atoms, the dashed lines hydrogen-bond interactions. Distances are in angstroms.

structure 6a between gas phase and solvent, it is reasonable to assume that this is the case also for the structures with the hydroxide groups out of the plane. We have therefore not optimized the geometries using the CPCM model for structures 6b, 7b, and 9. The bond distances and the relative energies are given in Tables 4, 6, and 7. The square bipyramid structure is the most stable one in all three models, confirming our previous conclusions that the tetrahydroxide ion exists without coordinated water. This tendency is even enhanced if one allows the hydroxide groups to rotate out of the equatorial plane. An additional confirmation is given by the U–OH[–] bond distance in the pentahydroxide ion $\text{UO}_2(\text{OH})_5^{3-}$, structure 9 (Supporting

(26) Schreckenbach, G.; Hay, P. J.; Martin, R. L. *Inorg. Chem.* **1998**, *37*, 4442.

(27) Hay, P. J. *J. Chem. Phys.* **1993**, *79*, 5469.

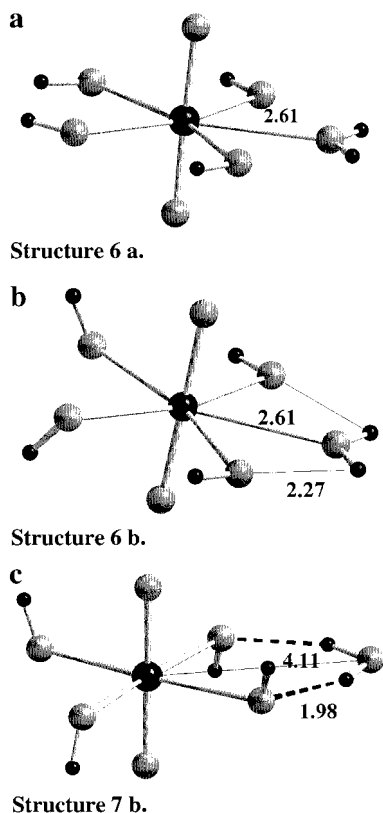


Figure 3. Uranium(VI) tetrahydroxide isomers in the gas phase with structures 6a (a), 6b (b), and 7b (c). The uranium and hydrogen atoms are black, and the oxygen atoms are medium gray. The thin lines denote distances between nonbonded atoms, the dashed lines hydrogen-bond interactions. Distances are in angstroms.

Information), where the CPCM model gives a value of 2.39 Å, much longer than the experimental value 2.26 Å. This planar structure represents a true energy minimum.

Comparison of the Structures of $\text{UO}_2(\text{OH})_4(\text{H}_2\text{O})^{2-}$ and $\text{UO}_2\text{F}_4(\text{H}_2\text{O})^{2-}$ in the Gas Phase. The EXAFS and crystal structure data reveal important differences between the two complexes (Tables 2 and 4); the tetrahydroxide ion has square bipyramid geometry while the tetrafluoride ion has pentagonal bipyramid geometry. This difference is not observed in the gas-phase calculations. Even the electronic populations in the 7s, 6p, 6d, and 5f are nearly identical, cf. Supporting Information Table S2. The U–L distances, $L = \text{F}^-$ or OH^- , are nearly the same in the most stable configuration of $\text{UO}_2\text{L}_4(\text{H}_2\text{O})^{2-}$, while the U– H_2O bond is longer in the fluoride complex. The U–F distance in the tetrafluoride complex, 2.26 Å, is the same as found by Schreckenbach et al.²⁸ and slightly longer than the 2.21 Å obtained by Pyykkö et al.²⁹ at the Hartree–Fock level. The gas-phase data cannot explain the experimentally observed differences in stoichiometry and structure in the solid state and in solution. We therefore assume that they are due to the influence of the solvent where the hydrogen bond interactions between the first and second coordination spheres play an important role.

Comparisons of Structure and Stability of $\text{UO}_2(\text{OH})_4(\text{H}_2\text{O})^{2-}$ and $\text{UO}_2\text{F}_4(\text{H}_2\text{O})^{2-}$ in a Solvent. The first model includes a specific second hydration sphere, restricted to the equatorial plane where the ligands are located. A model with a full second coordination shell would be too resource demanding.

We added three water molecules, keeping the total number equal to four, as shown in structures 10–15 (Supporting Information). The second coordination sphere affects both the metal–ligand bond distances and the relative energy of the isomers. The uranium–water distance decreases by 0.08 Å, while the U–(F, O) distance increases by at most 0.03 Å; cf. Tables 2/8 and 4/7, respectively. In the absence of solvent the isomer $\text{UO}_2(\text{OH})_4(\text{H}_2\text{O})^{2-}$ with a long U– H_2O distance (structure 7a) is 95.5 kJ/mol more stable than structure 6a with a short U– H_2O distance, as compared to 139.7 kJ/mol with a second coordination sphere of water (structures 13 and 14, Supporting Information), cf. Table 6. A change in the conformation of the OH groups is not expected to change this trend, as discussed above.

The corresponding tetrafluoride complexes structure 2 (Figure 2b) and structure 11 (Supporting Information) with noncoordinated water are respectively 138.8 and 83.7 kJ/mol more stable than the one with coordinated water (Table 3). In the solvent the relative stability of the $\text{UO}_2\text{L}_4(\text{H}_2\text{O})^{2-}$ complexes with a coordinated water decreases for $L = \text{OH}^-$ and increases for $L = \text{F}^-$. Although the five-coordinated structure is stabilized by the second coordination shell relative to the four-coordinated structure in the fluoride complex while it is destabilized in the hydroxide complex, the solvent model with a specific second coordination sphere cannot describe the experimentally observed difference between hydroxide and fluoride complexes. However, the model shows that all complexes are stabilized by hydrogen bonding to water in the second coordination sphere. Using 2.0 Å as an upper limit for a weak hydrogen bond interaction,³⁰ we have six and eight hydrogen bonds in the tetrafluoride structures 10 and 11 (Supporting Information) and four and two hydrogen bonds in the hydroxide complexes in structures 13 and 14 (Supporting Information), respectively. The number of hydrogen bonds is always smaller in the hydroxide complexes, and there is no evidence for hydrogen bond donation from the hydroxide, as judged from the $\text{OH}\cdots\text{O}$ distance of 3 Å, or longer. The *intramolecular* $\text{F}\cdots\text{H}$ distance in structures 10–12 is 2.40 Å, much longer than the *intermolecular* $\text{H}\cdots\text{F}^-$ distances. These findings support our suggestion that differences in hydrogen bonding make an important contribution to the observed difference between gas-phase and solution properties of the hydroxide and fluoride complexes. The solvent models used are rather primitive; more precise conclusions will require a model with a complete second coordination sphere with additional water molecules located above and below the equatorial plane. There are a total of 10 such positions in $\text{UO}_2\text{F}_4(\text{H}_2\text{O})^{2-}$, as compared to eight in $\text{UO}_2\text{F}_4^{2-}$. By just counting hydrogen bonds, one is led to the conclusion that a complete second coordination shell should stabilize the five-coordinated fluoride complex relative to the four-coordinated one.

The complexes have also been studied using a continuum model with spherical and shape-adapted cavities. The potential energy surface of structure 1 in the continuum model showed that bond distances are not strongly affected by the model: the bond distances change by 0.02 Å for the metal–ligand bonds and 0.03 Å for the internal uranyl distance. Reoptimizing the geometry lowers the total energy by only 4.2 kJ/mol, and we therefore used single-point calculations of the total energy at the gas-phase geometry to obtain the results given in Table 3. We found structure 1 with coordinated water in the first shell to be 3.9 kJ/mol more stable than structure 2. These results must be used with caution since the radius of the cage used varies

(28) Schreckenbach, G.; Hay, P. J.; Martin, R. L. *J. Comput. Chem.* **1999**, 20, 70.

(29) Pyykkö, P.; Li, J.; Runeberg, N. *J. Phys. Chem.* **1994**, 98, 4809.

(30) Hamilton, W. C.; Ibers, J. A. *Hydrogen bonding in solids*, W. A. Benjamin, Inc. New York, 1968.

Table 6. Relative Stability of the Three Isomers of $\text{UO}_2(\text{OH})_4(\text{H}_2\text{O})^{2-}$ in the Gas Phase and in the Solvent^a

complex	method	$\text{UO}_2(\text{OH})_4(\text{H}_2\text{O})^{2-}$		
		coordinated water	water in the plane at long distance	water out of the plane at long distance
bare complex	structure no.	6	7	8
	gas phase	0.00	-95.5	-44.5
	gas phase, hydroxide trans position	0.00	-134.4	
	spherical cavity	0.00	-11.8	22.1
	single point (cavity size)			
	CPCM single point	0.00	-12.0	+22.2
complex + second coordination shell	CPCM geom opt	0.00	-8.47	-7.78
	structure no.	13	14	15
	gas phase	0.00	-139.7	-39.2
	CPCM single point ^b	0.00	-68.8	-9.1

^a All energies in kJ/mol were calculated at the MP2 level. ^b Energies at the SCF level as MP2 calculations could not be handled.

Table 7. Optimized Geometry of $\text{UO}_2(\text{OH})_4(\text{H}_2\text{O})^{2-}$ with an Explicit Second Coordination Shell^a

chemical species	complex	U–O _{yl} (Å) [OUO]	U–O _{hydrox} (Å)	U–H ₂ O (Å)	U–H ₂ O second (Å)	OH...OH ₂ (Å)	HO...HOH (Å)
$\text{UO}_2(\text{OH})_4(\text{H}_2\text{O})\cdot(\text{H}_2\text{O})_3^{2-}$	struct 13 (C _{2v})	1.731 [179.9]	2.372–2.457	2.595	4.947–5.738	1.771	3.22–3.48
$\text{UO}_2(\text{OH})_4\cdot(\text{H}_2\text{O})_4^{2-}$ (four water molecules at long distance)	struct 14 Fig. 5a (C _{2h})	1.744 [180.0]	2.368–2.371	-	4.712	1.770	3.16
$\text{UO}_2(\text{OH})_4(\text{H}_2\text{O})\cdot(\text{H}_2\text{O})_3^{2-}$ (one water out of the plane at long distance)	struct 15 (C _{2v})	1.734 [177.8]	2.286–2.430	4.540	4.906–5.746	1.793	3.32–3.96

^a The different structures are shown in Figure 5a and the Supporting Information.

Table 8. Optimized Geometries for the $\text{UO}_2\text{F}_4(\text{H}_2\text{O})^{2-}$ with a Second Coordination Shell^a

chemical species	complex (sym)	U–O _{yl} (Å) [OUO]	U–F (Å)	U–H ₂ O (Å)	U–H ₂ O second (Å)	F...HOH (Å)
$\text{UO}_2\text{F}_4(\text{H}_2\text{O})\cdot(\text{H}_2\text{O})_3^{2-}$	struct 10 (C _{2v})	1.726 [178.0]	2.291–2.326	2.661	4.178–4.184	1.82–1.98 2.386 ^b
$\text{UO}_2\text{F}_4\cdot(\text{H}_2\text{O})_4^{2-}$ (four water molecules at long distance)	struct 11 (C _{2h})	1.720 [180.0]	2.27		4.030	2.00
$\text{UO}_2\text{F}_4(\text{H}_2\text{O})\cdot(\text{H}_2\text{O})_3^{2-}$ (one water out of the plane at long distance)	struct 12 (C _{2v})	1.730 [179.9]	2.252–2.279	4.550	4.027–4.041	2.00

^a The different structures are shown in the Supporting Information. ^b Intramolecular F...H.

by more than 1 Å between the different complexes in order to match the different sizes of the first coordination sphere. Thus, the interaction between the solute and the solvent should be stronger in the most compact structure, structure 1, than in the ones with long U–water distances. The cavity size is a smaller problem when we consider an explicit second coordination sphere model. Since all isomers then have about the same spatial extension, the cavitation energy is approximately constant. With the SCF + PCM model in the Molcas 5 package, the four-coordinated structure 11 is always the most stable, cf. Table 3, this is not in agreement with experimental observations.

The disadvantage of using a spherical cavity can be avoided by using other solvent models with properly tailored solute cavities. We have chosen the CPCM model since analytical second derivatives are available only for this implementation. Moreover, Cosentino et al.³¹ have recently proven its efficiency in reproducing the structure and the thermodynamic properties on lanthanide aqua ions. We first carried out single-point calculations of the total energy of the fluoride complexes without a second coordination sphere and estimated correlation at the

MP2 level. The results (Table 3) show that the solvent corrections preferably stabilize the five-coordinated geometry; structure 1 is the most stable one in the CPCM model tested, in the single-point calculation by 39.9 kJ/mol and in the geometry-optimized model by 10.1 kJ/mol. The electrostatic repulsion between the solute and solvent in the CPCM model induces a shortening of the uranium–ligand distances, especially of the uranium–water distance (0.13 Å). We also tested the CPCM model with an explicit second coordination sphere, but did not reoptimize the geometry because of the excessive computational cost. Also in this case the five-coordinated $\text{UO}_2\text{F}_4(\text{H}_2\text{O})^{2-}$ was the most stable isomer by 9 kJ/mol, cf. Table 3.

Turning now to the tetrahydroxide complexes we find similar, but smaller, solvent effects. However, the four-coordinated complex is the most stable one in all models tested (Table 6 and discussion above). To conclude, the CPCM models are able to explain the experimentally observed differences in the stoichiometry of the uranium(VI) tetrafluoride and tetrahydroxide complexes.

There is some change in the population of the different bonding orbitals between the complexes, cf. Supporting Information Table S2 and the Discussion.

(31) Cosentino, U.; Villa, A.; Pieta, D.; Moro, G.; Barone V. *J. Phys. Chem. B* **2000**, *104*, 8001.

Table 9. Calculated and Experimental Bond Distances of the Isomers of $\text{UO}_2\text{F}_3(\text{H}_2\text{O})_2^{2-}$ with and without Symmetry Constraints and Relative Energies at the SCF and MP2 Levels^a

chemical species	complex (sym)	method	U–O _{yl} (Å) [OUO]	U–F (Å)	U–H ₂ O (Å)	H···F (Å)	$\Delta U(\text{MP2})$ (kJ/mol)
$\text{UO}_2\text{F}_3(\text{H}_2\text{O})_2^-(\text{aq})$		EXAFS, this study	1.80	2.25	2.47		
$\text{UO}_2\text{F}_3(\text{H}_2\text{O})_2^-$ (non-neighboring water molecules in the plane)	struct 16 (C_{2v})	SCF gas phase	1.737 [179.4]	2.217–2.243	2.681	2.074	0
$\text{UO}_2\text{F}_3(\text{H}_2\text{O})_2^-$ (non-neighboring water molecules out of the plane)	struct 17 Fig. 4a (C_{2v})	SCF gas phase	1.72 [179.4]	2.160–2.189	5.029	2.356	–16.5
$\text{UO}_2\text{F}_3(\text{H}_2\text{O})_2^-$ (non-neighboring water molecules)	struct 18 Fig. 4b (C_1)	SCF gas phase SCF + CPCM	1.737 [179.1] 1.740 [179.5]	2.199–2.237 2.226–2.237	2.753 2.568	1.910 2.594	–26.3 0
$\text{UO}_2\text{F}_3(\text{H}_2\text{O})_2^-$ (neighboring water molecules in the plane)	struct 19 Fig. 4c (C_{2v})	SCF gas phase	1.718 [175.4]	2.152–2.260	2.920	1.787	+14.0
$\text{UO}_2\text{F}_3(\text{H}_2\text{O})_2^-$ (neighboring water molecules out of the plane)	struct 20 (C_{2v})	SCF gas phase	1.726 [172.4]	2.148–2.230	2.974	2.296	+2.64
$\text{UO}_2\text{F}_3(\text{H}_2\text{O})_2^-$ (neighboring water molecules)	struct 21 (C_1)	SCF gas phase SCF + CPCM	1.730 [178.7] 1.738 [178.1]	2.173–2.247 2.216–2.235	2.648–4.230 2.601	1.718 2.400	–47.8 +5.50

^a The different structures are shown in Figure 4 and the Supporting Information.

Geometry and Energy of Formation of $\text{UO}_2\text{F}_3(\text{H}_2\text{O})_2^-$.

There are two geometric isomers of $\text{UO}_2\text{F}_3(\text{H}_2\text{O})_2^-$; in addition there are several possible orientations of the coordinated water, but no experimental information on their relative stability. We have estimated the relative energy of the isomers and their bond distances, where the latter can be compared with experimental EXAFS data. We optimized the structures at the SCF level without symmetry constraints and calculated the energy at the MP2 level, using models with and without solvent, cf. Table 9. Imposing symmetry constraints, forcing the water molecule into the equatorial plane increases the energy by 26 kJ/mol at the MP2 level. Interestingly, in the solvent the most stable structure is close to the gas-phase symmetry-constrained one. Several different gas-phase structures were studied with symmetry constraints. In some of these, the water molecules are bonded only weakly, or not at all, to the uranium center, cf. Figure 4a,c and Supporting Information. If no symmetry constraints are imposed, the isomer with nonadjacent water molecules (structure 18, cf. Supporting Information) has two coordinated water molecules in a cis position above the equatorial plane. The trans configuration turns out to have the same energy, the difference being less than 0.05 kJ/mol. This shows that the repulsion between the hydrogen of the water molecules is not strong, which is expected since they are not neighbors. The situation is different in the other isomer with two adjacent water molecules. In C_1 , one of the two water molecules leaves the first coordination shell and enters the second coordination sphere at a distance of 4.23 Å, playing both the role of strong hydrogen bond donor to the neighboring fluoride atom (1.71 Å) and the role of hydrogen bond acceptor to the other water molecule with a H···O distance of 2.02 Å, cf. Table 9 and Supporting Information. This structure is the most stable in the gas phase, 48 kJ/mol below structure 16 at the MP2 level. It is noteworthy that, with symmetry constraints, the O–U–O group bends distinctly, at most 8°, at the SCF level in the gas phase in structures 19 and 20. This bond becomes more linear when the solvent is included, structure 21, Supporting Information. The electron distribution is also different in the models with and without solvent, cf. Supporting Information Table S2. Structure 18, with alternating fluoride and water ligands and the water

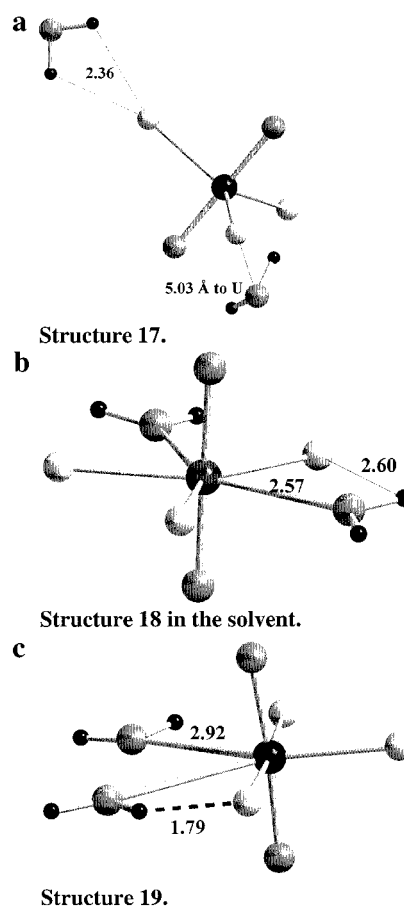


Figure 4. Uranium(VI) trifluoride isomers; structures 17 (a) and 19 (c) in the gas phase using C_{2v} symmetry and structure 18 (b) in the solvent without symmetry constraints. The uranium and the hydrogen atoms are black, the fluoride atoms light gray, and the oxygen atoms medium gray. Thin lines denote the distance between nonbonded atoms, the dashed lines hydrogen-bond distances. Distances are in angstroms.

plane perpendicular to the UO_2 axis (Figure 4b), is the most stable one in the CPCM model. The energy difference between structures 18 and 21 (Figure 4b and Supporting Information) is

only 5.50 kJ/mol, with almost no change in the U–water distance, 2.57 vs 2.60 Å. These differences are small and indicate that both isomers may be present in solution. The uranyl and the U–F distances are consistent with the experimental EXAFS values, while the U–water distance is 0.1 Å too long.

Geometry of $\text{UO}_2\text{F}_5^{3-}$. The $\text{UO}_2\text{F}_5^{3-}$ structure has been studied at the SCF level both in the gas phase and in the CPCM model. Only real frequencies were found at the equilibrium geometry. The CPCM model gives a U–F distance of 2.292 Å, which is not significantly different from the distances in the other fluoride complexes, or from the experimental EXAFS value, cf. Table 2.

Discussion

The following discussion is based on both the experimental and quantum chemical findings.

The Uranium(VI) Tetrafluoride Complex. The calculated U–F distance, 2.26 Å in the ground-state configuration of $\text{UO}_2\text{F}_4(\text{H}_2\text{O})^{2-}$ (structure 1), is in excellent agreement with the average value 2.27₅ Å, obtained from the EXAFS study. The theory-based U–OH₂ distance is 2.619 Å, significantly larger than the experimental value, 2.49 Å. This discrepancy is characteristic for aqua and hydroxide ligands, as observed both by us^{4,32} and Schreckenbach et al.²⁶ Structure data from solutions and theory thus gives concordant information on bond distances. These data have been used for a reinterpretation of the single-crystal X-ray structure determination of $\text{UO}_2\text{F}_4(\text{H}_2\text{O})^{2-}$ by Mak and Yip.² The crystal structure determination is precise, as indicated by the R_F value of 0.036. However, some of the bond distances (Table 2) differ significantly both from those deduced from theory and from the EXAFS data. We suggest that the uranium–water distance at 2.11 ± 0.07 Å from Mak and Yip is instead a uranium–fluoride distance. In view of the large standard deviation, this distance is not significantly different from those obtained by EXAFS and the wave function based calculations. Two other U–F distances, U–F(2), from Mak and Yip,² are 2.28 ± 0.01 Å, in good agreement with the values from EXAFS and theory. We suggest that the distance at 2.39 ± 0.01 Å that Mak and Yip² assigned to F(1) instead represents the average bond distance of one water and one fluoride, statistically distributed on the position 4(c) of the space group (*Im2m*). This average calculated from known structures is 2.36 Å.

The Uranium(VI) Trifluoride Complexes. The main difference between the C_1 and the symmetry-constrained C_{2v} geometry is in the *intramolecular* hydrogen bonding, which is much weaker in the higher symmetry, as indicated by the H···F distances of 2.07 Å in structure 16 and 1.91 Å in structure 18. In the presence of the solvent both isomers (structures 18 and 21) have a geometry close to the C_{2v} -constrained gas-phase structure, cf. Table 9. The relative energies of the different isomers indicate that the bonding energy of water to the uranium center in the different complexes is small and of the same order of magnitude as the hydrogen bonding. This is further substantiated by the small energy difference, 10 kJ/mol, between structures 17 and 18.

The relative energy and the U–H₂O and U–F[−] distances are nearly the same in the $\text{UO}_2\text{F}_3^-(\text{aq})$ isomers; hence it is not possible to distinguish them by using the EXAFS data. The experimental U–F[−] and U–OH₂ distances among $\text{UO}_2\text{F}_4^{2-}(\text{aq})$, $\text{UO}_2\text{F}_3^-(\text{aq})$, and $\text{UO}_2\text{F}_5^{3-}(\text{aq})$ are not significantly different.

Small differences in bond distances should appear as differences in the Debye–Waller factors; however, these are virtually the same in the three complexes. This information together with quantum chemical results on the small difference in energy between the different $\text{UO}_2\text{F}_3(\text{H}_2\text{O})_2^-$ isomers indicates that the solution complex $\text{UO}_2\text{F}_3^-(\text{aq})$ is a mixture of structures 18 and 21.

The distance between the water molecules in the second coordination sphere and the acceptor atoms, oxygen or fluorine in the first coordination sphere indicates very clearly the importance of *intermolecular* hydrogen bonding. On the other hand, the long donor–acceptor distance, 2 Å, or longer, between coordinated water and fluoride indicates that *intramolecular* hydrogen bonding is not important for the stabilization of the structures.

The Uranium(VI) Pentafluoride Complex. The EXAFS data from solution D contains a feature at 3.99 Å which may be interpreted as a U–U distance; the same feature, albeit weaker, can be seen also in solutions B and C. A U–U interaction implies the formation of a binuclear fluoride bridged complex as found in the solid state.³³ However, fluoride bridges have never been observed in solution.¹² Equilibrium constants determined by potentiometric methods do not vary with the total concentration of uranium; the same is true for the ¹⁹F NMR spectra,³⁴ and these observations provide strong evidence against the formation of binuclear complexes. The 3.99 Å peak may instead be the result of multiple scattering contributions.

The Uranium(VI) Tetrahydroxide Complex Revisited. The stoichiometry and structure of the uranium(VI) hydroxide complex formed in strongly alkaline solutions have been discussed by Clark et al.,¹ Wahlgren et al.,⁴ and Moll et al.,³ the results given in Table 6 show that the structure of $\text{UO}_2(\text{OH})_4(\text{H}_2\text{O})^{2-}$ with the lowest energy does not contain a bonded water molecules but has a square bipyramid geometry. The recalculated bond distance in $\text{UO}_2(\text{OH})_5^{3-}$ is in good agreement with the previous value from Wahlgren et al.,⁴ but much larger than the experimental EXAFS distance, confirming the stoichiometry proposed by Wahlgren et al. We tested the hydrogen bond donor capacity of the hydroxide in structure 14 by changing the position of the water molecules in the second coordination sphere so that the oxygen position was within bonding distance to the OH proton. No stable structure was obtained: the water molecules returned to the positions given in structure 14, cf. Figure 5a,b.

Chemical Bonding in the Fluoride and Hydroxide Complexes. The Mulliken charges (Table S2) of the different atoms in the fluoride complexes do not provide an indication of differences in bonding. The charge of F[−] is very near the same, −0.75, as are the charges of U and O_{y1}, 2.43 and −0.70, respectively. There is a slight redistribution of electrons in the uranyl unit between the $\text{UO}_2\text{L}_4(\text{H}_2\text{O})^{2-}$ complexes with a coordinated water, where the charges on uranium and oxygen in the fluoride and hydroxide systems are 2.43 (−0.68) and 2.47 (−0.73), respectively, where the larger charge separation indicates a more electrostatic bonding.

Conclusions

The theoretical calculations for $\text{UO}_2\text{L}_4(\text{H}_2\text{O})^{2-}$, L = F[−], OH[−], in the gas phase predict four-coordinated complexes. When solvent effects are included, theory predicts a four-coordinated hydroxide complex, with hydroxide ligands pointing out of the

(32) Farkas, I.; Bányai, I.; Szabó, Z.; Wahlgren U.; Grenthe, I. *Inorg. Chem.* **2000**, *39*, 799.

(33) Walker, S. M.; Halasyamani, P. S.; Allen, S.; O'Hare, D. *J. Am. Chem. Soc.* **1999**, *121*, 10513.

(34) Szabó, Z.; Glaser, J.; Grenthe, I. *Inorg. Chem.* **1996**, *35*, 2036.

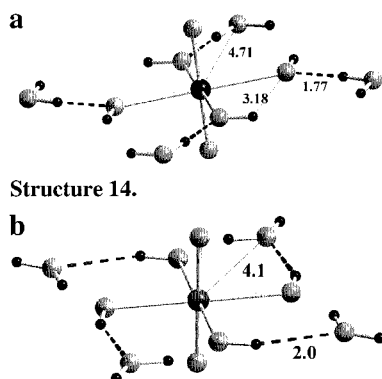


Figure 5. Uranium(VI) tetrahydroxide with a second coordination sphere with two different water positions (structure 14) (a, b). Uranium and hydrogen atoms are black, oxygen atoms medium gray. The thin lines denote distances between nonbonded atoms, the dashed lines hydrogen-bond distances. Distances are in angstroms. The second figure (b) shows the starting position when we investigated the hydrogen donor potential of the OH^- group.

equatorial plane, but a five-coordinated fluoride complex. The relative energy between gas phase and solvent for the tetra- and pentacoordinated complexes $\text{UO}_2\text{L}_4 \cdots (\text{H}_2\text{O})^{2-}$ and $\text{UO}_2\text{L}_4(\text{H}_2\text{O})^{2-}$ changes from -139 to $+9$ kJ/mol for the fluoride system and from -96 to -69 kJ/mol for the hydroxide system. These changes are large and result in the observed changes in coordination chemistry between the two ligands. Theory predicts $\text{UO}_2\text{F}_5^{3-}$ to exist in solution, with bond distances in good agreement with experiment. $\text{UO}_2(\text{OH})_5^{3-}$ is predicted not to be stable in solution, again in agreement with experimental observations. For $\text{UO}_2\text{F}_3(\text{H}_2\text{O})_2^-$, theory predicts the existence

of two isomers with very similar energy, and U–F bond distances in good agreement with experiments. The U–OH₂ distances are about 0.1 Å longer than the experimental observations, which is a normal result.

The gas-phase geometry is strongly influenced by *intramolecular* hydrogen bonding resulting in isomers with very different coordination geometry, differences that to a large extent disappear in the solvent models. These findings underscore the importance of including solvent effects when using quantum chemical methods for the study of chemical structure in solution.

The electron distribution in the various complexes is very similar, and the main change is a small redistribution of charge within the uranyl unit.

Acknowledgment. The EXAFS experiment was performed at the ROBL at ERSF in Grenoble and financially supported by EC under Contract HPRI-CT-1999-00077. The help of T. Reich, C. Henning, A. Rossberg, H. Funke, and M. Merroun during the XAS measurements is gratefully acknowledged. A generous grant from Carl Tryggers Stiftelse made it possible to buy the workstations needed for the quantum chemistry part. The support of the French Cotutelle program is gratefully acknowledged as are the computer resources provided by the University of Tromsø.

Supporting Information Available: The figures of all the structures not presented in the text (S1–S7) and all the coordinates of the computed structures in the gas phase and in the solvent (Table S1). The Mulliken atomic charges for the different compounds (Table S2). This material is available free of charge via the Internet at <http://pubs.acs.org>.

IC001405N